Covalent Sidewall Functionalization of Carbon Nanotubes by a "Formation−Degradation" Approach

Zhangquan Peng, Allan Hjarbæk Holm, Lasse Tholstrup Nielsen, Steen Uttrup Pedersen,* and Kim Daasbjerg*

Department of Chemistry and Interdisciplinary Nanoscience Center (iNANO), University of Aarhus, DK-8000 Aarhus C, Denmark

Received April 3, 2008. Revised Manuscript Received June 6, 2008

A diazonium salt-based strategy is employed to form a covalently attached multilayer of diphenyl disulfide on the surface of single-walled carbon nanotubes (SWCNTs) or multiwalled carbon nanotubes (MWCNTs). The interlayer S−S bonds are subsequently degraded reductively to produce essentially a single layer of thiophenols (or closely related derivatives) on the nanotube surface. The functionalization is achieved in what is effectively a one-pot procedure since the involved transformations are performed without intermediate workup. This "formation−degradation" modification approach is unique in the sense that it allows the generation of a thin well-defined molecular layer in spite of the involvement of highly reactive radicals in the first step. Transmission electron microscopy and thermogravimetric analyses support the approach proposed and reveal that a significant initial functionalization is achieved. In UV−vis spectroscopy, the disappearance of the Van Hove singularities of the SWCNT after the reaction is consistent with a covalent sidewall functionalization. Moreover, the resulting thin layer of thiophenols is reactive forming Au−S bonds with a macroscopic Au surface. Finally, the peripheral thiophenol groups of the MWCNT are employed as chemical linkers for anchoring gold nanoparticles and rods in a site-selective manner.

Introduction

Carbon nanotubes (CNTs) have attracted considerable attention from many different research fields due to their unique chemical and physical properties.[1] Sidewall functionalization using either noncovalently[2] or covalently based[3−7] strategies has provided a means of increasing the otherwise poor solubility of CNTs,[8] and helps in realizing some of the numerous potentials of CNTs. One attractive method for covalent functionalization is provided by in situ generated aryl diazonium salts.[9−13] Such species are easily converted into aryl radicals, and treatment of the CNTs can result in a highly functionalized material. However, because of the involvement of the reactive aryl radicals poorly defined and several nanometer thick polyaromatic multilayers are usually produced on the nanotube surface.[14]

In this paper we present an approach to overcome the problem of multilayer formation by using the principle of a "formation−degration" strategy recently developed for the modification of glassy carbon surfaces.[15] The basic idea is that an extensive multilayer of diphenyl disulfide is allowed to form on the surface of the CNT in a formation step through diazonium chemistry. However, since the multilayer contains cleavable S−S functionalities a subsequent chemical reductive degradation process can be carried out to remove the multilayer of disulfides without affecting the covalent (i.e., C−C bond) attachment of the layer to the CNT. In this manner, the resulting thin organic modification consisting of arylthiol groups is expected to be attached directly to the nanotube surface through C−C bonds, thus offering intimate contact between the two components.

To further underline the usability of the procedure, the functional arylic −SH anchor point is employed for the immobilization of two morphologically different gold metal species, namely, Au nanoparticles (Au NPs) and Au nanorods (Au NRs). The controlled deposition of gold matter on the sides of the functionalized CNTs offers a convenient protocol for the formation of CNT/nanoparticle hybrid materials. Such hybrid assemblies exhibit exciting collective properties that can be significantly different from those of the individual components and may eventually become the template of a

* Corresponding authors. E-mail: sup@chem.au.dk (S.U.P.) and kdaa@chem.au.dk (K.D.).

(1) Dresselhaus, M. S.; Dresselhaus, G.; Eklund, P. C. *Science of Fullerenes and Carbon Nanotubes*; Academic Press: New York, 1996.
(2) Britz, D. A.; Khlobystov, A. N. *Chem. Soc. Rev.* **2006**, *35*, 637–659, and refererences therein.
(3) Burghard, M.; Balasubramanian, K. *Small* **2005**, *1*, 180–192.
(4) Hirsch, A. *Angew. Chem., Int. Ed.* **2002**, *41*, 1853–1859.
(5) Niyogi, S.; Hamon, M. A.; Hu, H.; Zhao, B.; Bhowmik, P.; Sen, R.; Itkis, M. E.; Haddon, R. C. *Acc. Chem. Res.* **2002**, *35*, 1105–1113.
(6) Banerjee, S.; Hemraj-Benny, T.; Wong, S. S. *Adv. Mater.* **2005**, *17*, 17–29.
(7) Tasis, D.; Tagmatarchis, N.; Bianco, A.; Prato, M. *Chem. Rev.* **2006**, *106*, 1105–1136.
(8) Bahr, J. L.; Mickelson, E. T.; Bronikowski, M. J.; Smalley, R. E.; Tour, J. M. *Chem. Commun.* **2001**, 193–194.
(9) Dyke, C. A.; Tour, J. M. *J. Phys. Chem. A* **2004**, *108*, 11151–11159.
(10) Bahr, J. L.; Tour, J. M. *J. Mater. Chem.* **2002**, *12*, 1952–1958.
(11) Dyke, C. A.; Tour, J. M. *Chem. Eur. J.* **2004**, *10*, 812–817.
(12) Dyke, C. A.; Tour, J. M. *Nano Lett.* **2003**, *3*, 1215–1219.
(13) Dyke, C. A.; Tour, J. M. *J. Am. Chem. Soc.* **2003**, *125*, 1156–1157.
(14) Bahr, J. L.; Tour, J. M. *Chem. Mater.* **2001**, *13*, 3823–3824.
(15) Nielsen, L. T.; Vase, K. H.; Dong, M.; Besenbacher, F.; Pedersen, S. U.; Daasbjerg, K. *J. Am. Chem. Soc.* **2007**, *129*, 1888–1889.

10.1021/cm800954t CCC: $40.75
Published on Web 09/06/2008

number of applications ranging from electronic and optical sensors to catalytic materials.[16,17]

Several procedures have already been explored to synthesize such hybrid materials, including substrate-enhanced electroless deposition,[18,19] hydrophobic interactions,[20,21] covalent side-wall functionalization,[22−24] and spontaneous reduction.[25,26] Our "formation-degradation" procedure is simple and unique for radical-based processes in the sense that (a) it is possible to produce very thin functionalized layers through the reductive cleavage, (b) the outer-tube peripheral −SH groups allow for effective, facile, and site-selective means for the deposition of gold on the sides of the CNT,[27,28] and (c) the thin layer ensures that the metal materials are sure to be in intimate contact with the nanotube through, principally, a single molecular and covalently anchored "$-C_6H_4S-$" bridge.[29] This also separates our procedure from the approach developed by Harnisch et al.,[30] in which the linker (formed by electroreducing mercapto benzenediazonium salt) between a glassy carbon surface and Au NPs no doubt consists of a multilayer of thiolbenzene groups.

Experimental Section

Chemicals and Materials. The multiwalled CNTs (MWCNTs, Shenzhen Nanotech Port Co.) were purified and cut according to the procedure by Liu et al.,[27] and the single-walled CNTs (SWCNTs, HiPco, Carbon Nanotechnology Inc.) were purified by oxidation in an open pan at 300 °C for 1 h followed by reflux in concentrated HCl overnight. The material was then centrifuged and washed several times with water. The bis(4-aminophenyl) disulfide, cetyltrimethylammonium bromide (CTAB), triphenylphosphine, hydrogen tetrachloroaurate trihydrate, ascorbic acid, silver nitrate ($AgNO_3$), 4-aminothiophenol, sodium nitrite, and sodium borohydride were purchased from Aldrich and used as received. *N*,*N*-Dimethylformamide (DMF) and acetonitrile (MeCN) were from Labscan. Water was triple distilled. The Teflon (PTFE, pore size 0.45 μm) filters were from Sterlitech Corp. (PTFE04525100), the copper coated carbon grid (Cu-400CK, 400 mesh) from Pacific Grid, and the 1 mm diameter disk polycrystalline Au electrode from Cypress Systems (EE046).

Procedures and Instrumentation. *Functionalization of MWCNT and SWCNT.* Twelve milligrams of MWCNTs were mixed with 250 mg of bis(4-aminophenyl) disulfide (1 mmol) in 25 mL of 1.0 M aqueous HCl solution and sonicated (Branson 1510, 70 W power, Bransonic Ultrasonic Corporation) overnight. The dispersion was then cooled to 0 °C and stirred for 10 min followed by dropwise addition of 140 mg of $NaNO_2$ (2 mmol) in 5 mL of H_2O at 0 °C. The reaction solution was kept at 0 °C for 30 min, then heated to 40 °C for 2 h, and cooled to room temperature. The reductive degradation was accomplished either by addition of 50 mL of 1.0 M HCl and 260 mg of Ph_3P (1 mmol) with stirring for 1 h or by dilution with 50 mL of ethanol and addition of 40 mg of $NaBH_4$ (1 mmol) and 50 mL of 1.0 M HCl with stirring for 1 h. In general, we found no significant differences between the final products regardless of the employed degradation procedure.

The SWCNTs (12 mg) were mixed with bis(4-aminophenyl) disulfide (250 mg) in 25 mL of 1.0 M HCl aqueous solution and sonicated overnight. The dispersion was then cooled to 0 °C and stirred for 10 min followed by dropwise addition of 140 mg of $NaNO_2$ (2 mmol) in 5 mL of H_2O at 0 °C. The reaction solution was kept at 0 °C for 30 min, then heated to 40 °C for 2 h, and cooled to room temperature. The reductive degradation was carried out by diluting the mixture with 25 mL of MeCN and 25 mL of ethanol, and under stirring 260 mg of Ph_3P (1 mmol) and 25 mL of 1.0 M HCl were added. Stirring was continued for 1 h.

The reaction solutions were filtered through a PTFE membrane. The filtrates were dispersed in 50 mL of water by sonication and filtered. The procedure was repeated three times and then also performed with ethanol (50 mL) three times. At this point no further changes could be observed in our analyses. Moreover, similar results were obtained if DMF was used in the cleaning procedure. It is therefore assumed that any organics left on the surface are indeed covalently attached. Finally, the product was collected and dried in vacuum.

To deposit gold on the CNT surface, the functionalized MWCNT (0.5 mg) was first dispersed in 2 mL of aqueous 0.1 M CTAB by sonication for 30 min. Solutions of Au NPs were prepared by mixing 50 μL of aqueous 50 mM $HAuCl_4$, 7.5 mL of aqueous 0.1 M CTAB, and 600 μL of aqueous 10 mM $NaBH_4$.[31−33] To immobilize the nanoparticles onto the MWCNT-PhSH, 9 μL of the Au NP solution was added to 2 mL of MWCNT-PhSH dispersion with stirring for 30 min. For the seeded growth of the Au NPs on the MWCNT-PhS-Au NP hybrid to form MWCNT-PhS-Au NRs, 9 μL of the Au NP solution was added to the 2 mL of MWCNT-PhSH dispersion and then poured into a 3 mL growth solution (taken from a mixture of aqueous solutions of 40 μL of 50 mM $HAuCl_4$, 4.75 mL of 0.1 M CTAB, 12 μL of 10 mM $AgNO_3$, and 32 μL of 0.1 M ascorbic acid).[31−33]

The Au NRs were prepared by addition of 9 μL of the Au NP solution into a 3 mL growth solution prepared as described above.[31−33] Assembly of the preformed Au NRs on the MWCNT-PhSH was performed by stirring for 30 min a mixture of 0.1 mL Au NRs solution and 2 mL of the MWCNT-PhSH dispersion. The products were isolated by centrifugal sedimentation (10 000 rpm, 10 min), washed with water, and centrifuged three times.

(16) Wildgoose, G. G.; Banks, C. E.; Compton, R. G. *Small* **2006**, *2*, 182–193.
(17) Katz, E.; Wilner, I. *ChemPhysChem* **2004**, *5*, 1084–1104.
(18) Li, J.; Moskovits, M.; Haslett, T. *Chem. Mater.* **1998**, *10*, 1963–1967.
(19) Qu, L.; Dai, L.; Osawa, E. *J. Am. Chem. Soc.* **2006**, *128*, 5523–5532.
(20) Mieszawska, A. J.; Jalilian, R.; Sumanasekera, G. U.; Zamborini, F. P. *J. Am. Chem. Soc.* **2005**, *127*, 10822–10823.
(21) Ellis, A. V.; Vijayamohanan, K.; Goswami, R.; Chakrapani, N.; Ramanathan, L. S.; Ajayan, P. M.; Ramanath, G. *Nano Lett.* **2003**, *3*, 279–282.
(22) Li, X.; Liu, Y.; Fu, L.; Cao, L.; Wei, D.; Wang, Y. *Adv. Funct. Mater.* **2006**, *16*, 2431–2437.
(23) Zanella, R.; Basiuk, E. V.; Santiago, P.; Basiuk, V. A.; Mireles, E.; Puente-Lee, I.; Saniger, J. M. *J. Phys. Chem. B* **2005**, *109*, 16290–16295.
(24) Shi, J.; Wang, Z.; Li, H.-L. *J. Nanopart. Res.* **2006**, *8*, 743–747.
(25) Choi, H. C.; Shim, M.; Bangsaruntip, S.; Dai, H. *J. Am. Chem. Soc.* **2002**, *124*, 9058–9059.
(26) Kim, D. S.; Lee, T.; Geckeler, K. E. *Angew. Chem., Int. Ed.* **2006**, *45*, 104–107.
(27) Liu, J.; Rinzler, A. G.; Dai, H.; Hafner, J. H.; Bradley, R. K.; Boul, P. J.; Lu, A.; Iverson, T.; Shelimov, K.; Huffman, C. B.; Rodriguez-Macias, F.; Shon, Y.-S.; Lee, T. R.; Colbet, D. T.; Smalley, R. E. *Science* **1998**, *280*, 1253–1256.
(28) Coleman, K. S.; Bailey, S. R.; Fogden, S.; Green, M. L. H. *J. Am. Chem. Soc.* **2003**, *125*, 8722–8723.
(29) Dyke, C. A.; Stewart, M. P.; Maya, F.; Tour, J. M. *Synlett* **2004**, *1*, 155–160.
(30) Harnisch, J. A.; Pris, A. D.; Porter, M. D. *J. Am. Chem. Soc.* **2001**, *121*, 5829–5830.
(31) Gou, L.; Murphy, C. J. *Chem. Mater.* **2005**, *17*, 3668–3672.
(32) Murphy, C. J.; Sau, T. K.; Gole, A. M.; Orendorff, C. J.; Gao, J.; Gou, L.; Hunyadi, S. E.; Li, T. *J. Phys. Chem. B* **2005**, *109*, 13857–13870.
(33) Orendorff, C. J.; Murphy, C. J. *J. Phys. Chem. B* **2006**, *110*, 3990–3994.

UV−Vis Analysis. UV−vis absorption spectra were recorded in DMF solutions on a Shimadzu UV-3600 UV−vis spectrophotometer using the pure solvent as background.

TEM Analysis. A Philips CM 20 bright-field transmission electron microscopy operated at an acceleration voltage of 200 kV was used for TEM analysis. The samples were prepared by placing a droplet of ~0.1 mg mL^{-1} solution of the material on a copper coated carbon grid followed by air-drying.

TGA Analysis. Thermogravimetric analysis (TGA) was performed with a Mettler TGA Instrument. The ramp was 20 °C min^{-1}, and the curves were recorded under a working N_2 flux equal to 50 mL min^{-1} in the range of 25−800 °C. The measurements were carried out on carefully dried, accurately weighed 2−4 mg samples in an open platinum pan.

XPS Analysis. XPS analysis was recorded with a SSX-100 X-ray photoelectron spectrometer (Surface Science Laboratories, U.S.A.), with an Al Kα X-ray source (1487 eV) at a power of approximately 150 W. The pass energy for survey scans was 200 keV. The pressure in the main chamber during the analysis was in the range of 10^{-8} mbar. Atomic concentrations of the elements were calculated by determining the relevant integral peak intensities using a linear type background. The systematic error is estimated to be of the order of 5−10%. The XPS powder samples were prepared by immobilizing the dry CNT material on the one side of a piece of double sided tape. The tape was found not to interfere with the measurements. During the acquisition, the instrument was operated in the charge neutralization mode to minimize sample charging.

Electrochemical Analysis. For the electrochemical experiments a CHI 900 electrochemical workstation was used. The working electrode was a 1 mm diameter disk polycrystalline Au electrode. Before use the electrode was polished by hand using 0.05 μm alumina slurry and sonicated in water. A Pt wire served as the counter electrode while a Ag/AgCl electrode was employed as the reference electrode. Solutions were deaerated with argon and kept under an argon atmosphere during the experiments.

To remove any organic material before the immobilization of thiols, the electrode was cleaned electrochemically in 0.5 M H_2SO_4 by potential cycling between −0.2 and 1.5 V vs Ag/AgCl until a reproducible voltammogram was obtained. The electrode was then rinsed in water and ethanol and immediately immersed in ethanolic solutions of either 0.1 mg mL^{-1} MWCNT-PhSH or SWCNT-PhSH or 1 mM 4-aminothiophenol for 24 h. Finally, the electrode was rinsed carefully with ethanol and water.

The total charge, Q, used for the reduction of the Au−S bonds was obtained by coulombmetric integration of the background-subtracted electrochemical response recorded in cyclic voltammetry in 0.1 M NaOH at a sweep rate of 0.1 V s^{-1}. A linear background was assumed and manually adjusted under the faradic peak. The surface coverage, Γ, was calculated using Faraday's law, that is, $\Gamma = Q/nFA$, where n is the number of electrons transferred, F is Faraday's constant, and A represents the geometric area of the electrode.

Results and Discussion

CNTs subjected to functionalization by in situ generated arenediazonium species are expected to carry a several nanometer thick arylic multilayer on the surface. The mechanism has been suggested to proceed through the generation of highly reactive aryl radicals by self-catalysis by the nanotubes.[29] The radicals then add onto the conjugated sp^2-hybridized framework constituting the CNTs and, in particular, defect sites.[7−14,29] While the extent of functionalization and density to some degree may be controlled by parameters such as temperature, concentration, and solvent,[12] the continued production of aryl radicals inevitably leads to an unordered material due to the aryl radicals reacting not only with the CNT surface but also with initially formed layers.

In a previous paper we presented a "formation-degradation" protocol, in which a few nanometer thick, unordered multilayer of diphenyl disulfides was first built on a glassy carbon surface using electrochemistry followed by a controlled electrochemical degradation of the interlayer S−S bonds.[15] The degraded film is of a comparatively more well-defined geometry, and any material attached to the surface via peripheral thiol groups is expected to be connected to the electrode surface through covalent bonds.[34] We were also able to show that the film properties could be switched electrochemically between the nucleophilic thiophenolate and the electrophilic disulfide forms.

Herein, we were interested in pursuing these findings for developing the controlled radical-based functionalization of CNTs and the site-selective deposition of gold material. As others have shown,[6,16,17,23,24,28] the formation of peripheral nanotube −SH groups provides an excellent means for the immobilization of Au NPs and Au NRs. Thus, we were interested in investigating to what extent the use of the "formation−degradation" protocol would allow for the production of a thin thiophenol film to provide a basis for the site-selective deposition of gold matter. Our procedure is essentially a one-pot procedure since all the involved transformations may be carried out without intermediate workup.

The overall concept of the approach is outlined in Scheme 1. It centers on the initial formation of an extensive polymeric layer of diaryl disulfide through a spontaneous grafting process involving the pertinent in situ generated diazonium salt in aqueous solution. As discussed in detail elsewhere for the modification of glassy carbon surfaces, the polymerization reaction is expected to occur mainly through the "outer" aryl ring.[15,34] A subsequent reductive cleavage of the interlayer S−S bonds using Ph_3P or $NaBH_4$ removes the extensive multilayer of disulfides without affecting the far stronger C−C bonds that are formed between the CNT and the innermost layer of the arylic film. Overall the procedure

(34) In an ongoing study we are working on clarifying the type of molecular structures left in the film after reductive degradation. It is relatively safe to assume that the degradation process cleaves S−S bonds and not the far stronger C−C bonds that are formed between the surface and the arylic film. Moreover, since the film was formed with aryl radicals, the multilayers may be connected through not only S−S but also C−C, e.g.,−S−Ph−Ph−S−, and C−S bonds, e.g.,−S−Ph−S−Ph−. By taking such considerations into account, the degradation, most probably, provides a thin film constituted of individual thiophenolates in addition to biphenylbis(thiolate) and (phenylthio)benzenethiolate, this also being a result in accordance with the layer thicknesses measured by AFM.[15] Throughout the rest of the paper, we will use the term "thiophenol film" to signify a thin layer made up of individual thiophenols but also some biphenyldithiol and (phenylthio)benzenethiol. It should also be mentioned that the use of two different aryl-substituted salts, i.e., 4,4′-disulfanediyldibenzenediazonium and 4-[(4-chlorophenyl)disulfanyl]benzenediazonium, led to similar film formation independent of the substituent on the outer ring.[15] For the former salt, which is employed in this study, this implies that the second N_2^+ group has no specific function and most likely simply is reduced off and replaced with a hydrogen atom during the modification procedure.

Scheme 1. Functionalization of MWCNTs and SWCNTs by the "Formation−Degradation" Approach, including the Pristine CNTs and the Multilayered (A) and the Degraded Materials (B)

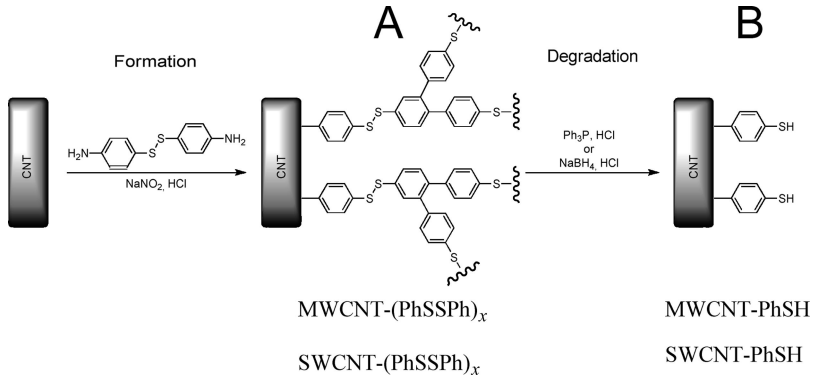

should thus lead to the covalent sidewall functionalization of the CNTs with a thin layer of thiophenols.

Characterization of the Sidewall-Functionalized CNTs. *TEM Experiments.* Figure 1 illustrates the TEM images obtained on the diphenyl disulfide functionalized MWCNT [MWCNT-$(PhSSPh)_x$] and SWCNT [SWCNT-$(PhSSPh)_x$] and the degraded thiophenol functionalized MWCNT (MWCNT-PhSH) and SWCNT (SWCNT-PhSH). Interestingly, if MWCNT-$(PhSSPh)_x$ or SWCNT-$(PhSSPh)_x$ are isolated prior to the reductive cleavage, the formation of the polyaromatic layer on the surface can easily be observed (marked by the circles in Figure 1). Equally notable, the multilayer would appear not to be uniformly distributed along the backbone of the nanotube. Presumably, the polyaromatic coating starts growing from defect sites, and once the first aryl group has become attached it is more reactive toward secondary incoming aryl radicals than the pristine CNT structure along the backbone. The result would be the growth of "mushrooms" on the CNT surface; very much resembling what is also seen with the electrochemical surface derivatization of glassy carbon surfaces.[35]

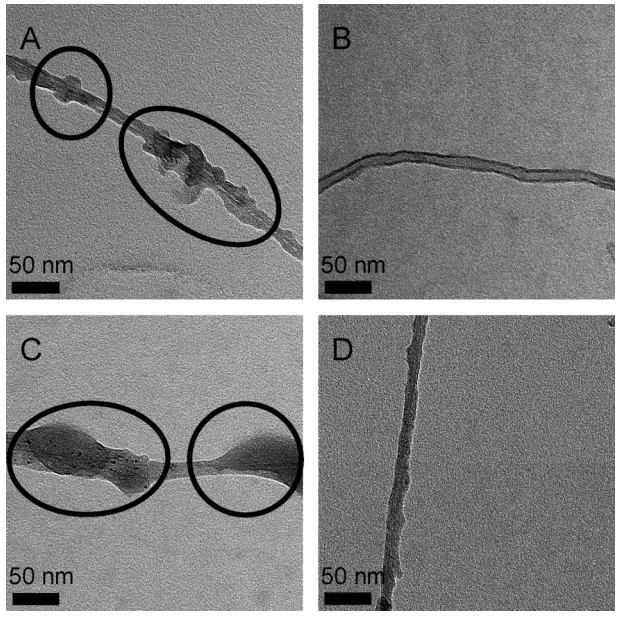

Figure 1. TEM images of MWCNT-$(PhSSPh)_x$ (A), MWCNT-PhSH (B), SWCNT-$(PhSSPh)_x$ (C), and SWCNT-PhSH (D), respectively. The circles mark sites of multilayered polymer sidewall functionalization.

However, once the nanotubes have been treated with the multilayer degradant in the second step, they show no clear differences compared to the pristine nanotubes; that is, the extensive polyaromatic network is released by reductive cleavage of S−S bonds leaving only those groups that are directly linked to the tubes through C−C bonds.[34] Such a microscopic inspection of the materials does clearly not allow for a quantitative means to estimate the extent of functionalization, in particular, if the functionalization of SWCNTs occurs on bundles rather than individualized units as suggested by the relatively large radius of SWCNT-PhSH in Figure 1D (compare also with Figure 1B).[12] It does, however, lend visual support to the intended "formation−degradation" mechanism.

TGA Experiments. To estimate the extent of surface functionalization on the CNTs, thermogravimetric analysis was employed (Supporting Information, Figure S1). A TGA mass loss of about 14% was measured up to a temperature of 600 °C for MWCNT-$(PhSSPh)_x$ whereas MWCNT-PhSH provided a loss of only 3%. At higher temperatures several further mass step losses were observed, but they are less reliable as the CNT starts to decompose at temperatures of 6−700 °C.[36,37] Importantly, in the lower temperature range (T < 600 °C) a pristine MWCNT sample exhibited a mass loss of less than 1%.

The mass loss of MWCNT-PhSH may be calculated to correspond to an estimated functionalization in every 1 in 300 of the multiwall nanotube carbons.[38] This translates into a functionalization fraction of 0.4%. At first sight our findings suggest a very limited degree of functionalization. However,

(35) Holm, A. H.; Møller, R.; Vase, K. H.; Dong, M.; Besenbacher, F.; Pedersen, S. U.; Daasbjerg, K. *New. J. Chem.* **2005**, *29*, 659–666.
(36) Chen, C.-M.; Chen, M.; Peng, Y.-W.; Yu, H.-W.; Chen, C.-F. *Thin Solid Films* **2006**, *498*, 202–205.
(37) Sengupta, R.; Ganguly, A.; Sabharwal, S.; Chaki, T. K.; Bhowmick, A. K. *J. Mater. Sci.* **2007**, *42*, 923–934.
(38) The fraction of carbons in the MWCNT-PhSH or SWCNT-PhSH materials that have been functionalized is calculated from the percent mass loss (Δm) by the following formula: $\Delta m = 109/(n \times M_C + 109)$, where n represents the number of carbons on the nanotube for each of the thiophenol groups and M_C the molecular mass of carbon (for SWCNT-PhSH the mass loss is corrected for that of pristine SWCNT). The number of disulfide layers x in MWCNT-$(PhSSPh)_x$ or SWCNT-$(PhSSPh)_x$ can be calculated from Δm and the mass loss of disulfide film, $\Delta m_x = 216x/(n \times M_C + 216x)$.

considering that most of the sidewall carbons of MWCNTs are chemically inaccessible,[13] the implication may be a considerable functionalization of the outermost carbon shell. The mass loss appears nonetheless to be quite low when one considers the TEM image of MWCNT-(PhSSPh)$_x$ (Figure 1A) which showed regions of extensive multilayer functionalization. It is difficult to estimate the average number of layers in the MWCNT-(PhSSPh)$_x$ material, that is, the value of x, by TEM due to the inhomogeneity of the modification as well as the MWCNT material. On the other hand, MWCNT-PhSH (Figure 1B) has relatively smooth sidewalls and cannot be distinguished from the pristine CNT. It therefore seems reasonable that a mass loss of only 3% was observed with this material.

The SWCNT-(PhSSPh)$_x$ sample exhibited a mass loss of around 27% for temperatures up to 600 °C and 15% for the reductively degraded SWCNT-PhSH. When a pristine SWCNT sample was subjected to the same analysis, a loss of approximately 4% was observed, presumably due to degassing and solvent evaporation. When the mass loss of the pristine sample is accounted for, an estimated 1 in every 70 carbons has been functionalized which translates into a functionalization fraction of 1.4%. Under the assumption that the SWCNT-PhSH carries close to a single layer of the arylic film on the surface,[34] the mass loss difference before and after degradation can be used to estimate the number of disulfide layers x in SWCNT-(PhSSPh)$_x$ material, that is, $x = 1-1.5$ corresponding to $2-3$ "$-C_6H_4S-$" units. It is important to emphasize that this is an average number and that for heavily functionalized regions as seen in Figure 1C, x can easily be larger.

The outlined stoichiometric ratios are not far from what has been reported in similar procedures in the literature for SWCNT[13,14,39,40] and MWCNT,[13,41] and they are as expected significantly larger for the SWCNT compared to the MWCNT (when they are subjected to the same treatment) due to the larger diameter of the MWCNT and the fact that some of the sidewalls of the MWCNT are chemically inaccessible.[13] When one considers the TEM images and, in particular, the visually quite extensive functionalization in Figure 1, the calculated ratios of the SWCNT may seem lower than expected. However, the functionalization is clearly not homogeneous and there might be regions of very modest functionalization, if any. One may assume that the reason for inhomogeneity can be ascribed to the aforementioned "mushroom" growth of the polyaromatic film from defect sites.

XPS Experiments. To further characterize the materials and estimate the extent of surface functionalization, X-ray photoelectron spectroscopy was carried out. Table 1 outlines the pertinent atomic surface concentrations. Although not included in the table, the pristine MWCNT and SWCNT were also analyzed for comparison. The predominant signal (>95%) was carbon with a small percentage of oxygen (1−3%) in addition to trace amounts (<0.5%) of nitrogen, fluorine, and iron. The iron probably comes from incomplete removal of the catalyst used for their preparation, and the fluorine could arise from impurities introduced when filtering through the PTFE membrane.

Table 1. XPS Surface Elemental Compositions of the CNTs[a,b]

		surface atomic concentration, %		
entry		C	O	S
A	MWCNT-(PhSSPh)$_x$	89.1	6.0	2.2
B	MWCNT-PhSH	93.2	4.9	0.4
C	SWCNT-(PhSSPh)$_x$	74.2	10.1	11.5
D	SWCNT-PhSH	83.7	11.1	3.3

[a] In addition to the reported elements, the surfaces contain small traces of various impurities (see text). [b] The calculated concentrations express the total content of the particular atom.

After modification by the diphenyl disulfide groups (entries A and C), the MWCNT-(PhSSPh)$_x$ and SWCNT-(PhSSPh)$_x$ materials expectedly have a significant surface concentration of sulfur. The surface atomic concentration appears to be quite different for the MWCNT and SWCNT samples indicating that the SWCNTs are surface-functionalized to a significantly higher extent than the MWCNTs. This is not surprising and in line with the TGA results considering that the MWCNT is constituted of several layers of aromatic conjugated networks with some of them inaccessible for functionalization.

For MWCNT-(PhSSPh)$_x$ and SWCNT-(PhSSPh)$_x$ the polymeric nature of the multilayered functionalization makes it impossible to estimate the number of nanotube carbons for each S on the modification. It may be noted, however, that with the 11.5% obtained for SWCNT-(PhSSPh)$_x$ the atomic concentration of S is not far from the ~14% expected if the XPS analysis was performed on diphenyl disulfide solely (S/C ratio = 1/6).

After the degradation has been performed (entries B and D), the material has a lower concentration of sulfur on the surface, 0.4% for MWCNT-PhSH and 3.3% for SWCNT-PhSH, respectively. This again lends support to a modification mechanism in which most of the extensive polymeric layer has been removed and only relatively few of the nanotube carbons are functionalized by a phenylthiol group. In this connection it is interesting to note that the content of sulfur on the SWCNT surface before and after degradation, that is, 11.5 versus 3.3%, suggests that on average three to four layers of "$-C_6H_4S-$" groups are present on the SWCNT-(PhSSPh)$_x$ material calculated on the assumption that the SWCNT-PhSH carries only a single layer of aryl groups. These numbers correlate reasonably with the two to three layers of "$-C_6H_4S-$" groups on the SWCNT-(PhSSPh)$_x$ material estimated from TGA (vide supra).

The XPS results for the MWCNT-PhSH and SWCNT-PhSH materials can be compared with the corresponding TGA results. For MWCNT-PhSH the TGA experiments indicated that 1 in every 300 carbons of the material had been functionalized while a S/C ratio of ~1/250 is found from XPS. Also, from the TGA results, we estimated that on average 1 in 70 carbons of the SWCNT-PhSH material had been functionalized corresponding to a S/C ratio of ~1/

(39) Bahr, J. L.; Yang, J.; Kosynkin, D. V.; Bronikowski, M. J.; Smalley, R. E.; Tour, J. M. *J. Am. Chem. Soc.* **2001**, *123*, 6536–6542.
(40) Wang, S.; Liang, Z.; Liu, T.; Wang, B.; Zhang, C. *Nanotechnology* **2006**, *17*, 1551–1557.
(41) Basiuk, E. V.; Gromovoy, T. Y.; Datsyuk, A. M.; Palyanytsya, B. B.; Pokrovskiy, V. A.; Basiuk, V. A. *J. Nanosci. Nanotechnol.* **2005**, *5*, 984–990.

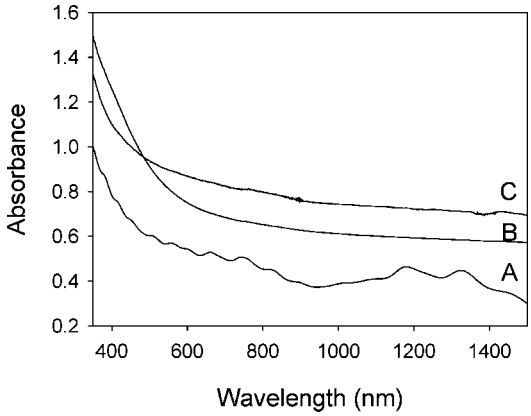

Figure 2. UV−vis absorption spectra of pristine SWCNT (A), SWCNT-(PhSSPh)$_x$ (B), and SWCNT-PhSH (C), respectively, in DMF.

76. From XPS the S/C ratio can be calculated to be ∼1/25. Considering the experimental uncertainties inherent to both techniques, these results seem reasonable. Moreover, parts of the SWCNT may have been functionalized as bundles instead of individual tubes, which would lead to a higher relative ratio of S to C in XPS (which scans the surface) as compared to the TGA (which examines the sample/structure as a whole).

UV−Vis Spectroscopy. UV−vis spectroscopy was also performed to characterize the sidewall functionalization of the SWCNTs. As may be observed in Figure 2 the absorption spectrum of pristine SWCNTs (spectrum A) shows the expected Van Hove singularities, whereas the spectra of the functionalized SWCNTs (spectra B and C) show only modest spectral fine structure in the same range. Such a dramatic attenuation of the Van Hove singularities is consistent with the occurrence of a covalent sidewall functionalization,[9−14,42] that is, disruption of the conjugated π system. It therefore further substantiates the involvement of aryl radicals in the covalent grafting process. If the modification had been noncovalent in nature the UV−vis spectrum would still have fine structure although not as distinct as seen for the pristine material.[11,14]

Electrochemical Desorption Experiments. The spontaneous self-assembly of organic thiols on noble metal surfaces leads to the formation of covalent metal−S bonds that can be electrochemically desorbed in alkaline solutions at modestly negative potentials. To verify the formation of "active" peripheral thiols on the surface of the reductively degraded MWCNT-PhSH and SWCNT-PhSH, we immobilized the thiolated CNTs on a Au surface and investigated the electrochemical response.

Figure 3A and B illustrates the current−potential curve of the MWCNT-PhS-Au and SWCNT-PhS-Au materials. In both cases a distinct reduction peak is observed at approximately −0.8 V versus Ag/AgCl characteristic of the reductive desorption of Au−S bonds.[43,44] After the first scan this reduction peak disappears completely, demonstrating that in our system there is little or no readsorption of the modifiers

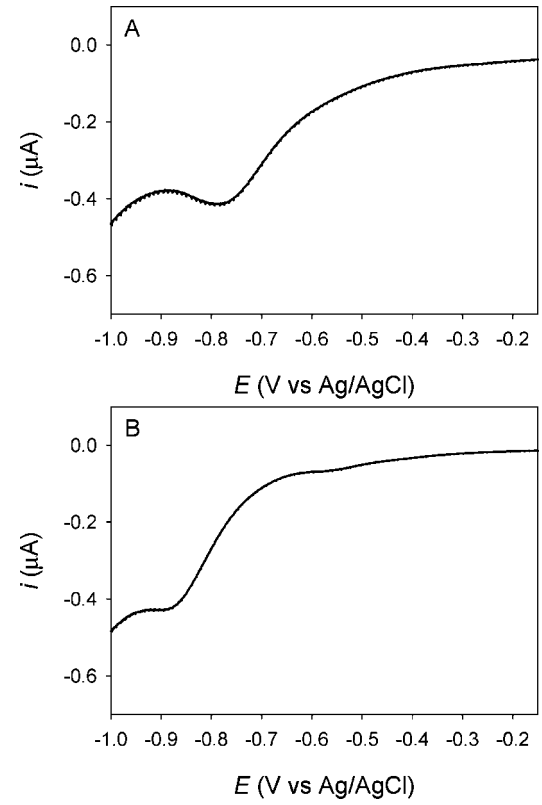

Figure 3. Linear sweep voltammogram of MWCNT-PhSH (A) and SWCNT-PhSH (B) functionalized Au electrode in 0.1 M NaOH solution, recorded at a sweep rate of 0.1 V s^{-1}.

occurring upon scan reversal in the positive direction. Interestingly, although disulfides are also expected to react with the Au surface, no peaks were observed in the pertinent electrochemical range for electrodes treated with either MWCNT-(PhSSPh)$_x$ or SWCNT-(PhSSPh)$_x$. The electrochemical peak values measured from the experiments in Figure 3 are also supported by the investigation of the model system 4-aminothiophenol (Supporting Information, Figure S2).

Overall the electrochemical signals allow us to identify the formation of a Au−S bond, that is, the functionalized nanotubes peripheral thiol groups are "active", and also to quantify the extent of layer formation by faradaic integration. The surface density of Au−S bonds for MWCNT-PhS-Au and SWCNT-PhS-Au was calculated to be 0.22×10^{-10} and 0.18×10^{-10} mol cm^{-2}, respectively, after correction for the background current.[44] This value should be compared to the saturated coverage of 3.0×10^{-10} mol cm^{-2} from the electrodesorption of 4-aminothiophenol layers.

Accordingly, we may therefore state that approximately 6−7% of the Au electrode surface was derivatized with thiol groups from the modified CNTs. Most probably, the nanotubes are lying flat down on the Au surface to maximize the number of Au−S bonds, although the ends of the tubes are expected to carry the highest relative functionalization.[1−7] Notwithstanding the variation of the tubing curvature and diameter between MWCNT and SWCNT it is interesting to note that comparable amounts of Au−S bonds are formed in both cases.

This appears to be somewhat contradictory to the characterization by TGA and XPS outlined above. However, as

(42) Price, B. K.; Tour, J. M. *J. Am. Chem. Soc.* **2006**, *128*, 12899–12904.
(43) Zhong, C.-J.; Porter, M. D. *J. Am. Chem. Soc.* **1994**, *116*, 11616–11617.
(44) Walczak, M. M.; Alves, C. A.; Lamp, B. D.; Porter, M. D. *J. Electroanal. Chem.* **1995**, *396*, 103–114.

Scheme 2. Principle of the Site-Selective Deposition of Au NPs and Au NRs[a]

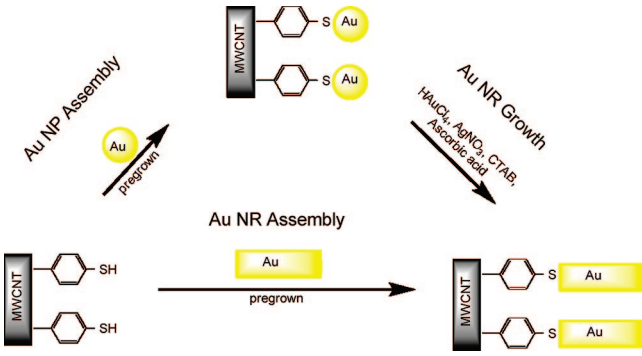

[a] The MWCNT-PhSH is treated with Au NPs followed by a seeded growth of the Au NPs into Au NRs or treated with preformed Au NRs.

noted earlier, the degree of functionalization of the outermost tube in the MWCNT may be equal or close to that of the SWCNT material. The electrochemical data seemingly support this view. Nevertheless, the curved nature of the CNTs makes it impossible for all the peripheral phenylthiols to become attached to the Au surface. Thus, it is important to emphasize that the electrochemical desorption data are not representative of the actual number of phenylthiol groups on the surface.

Formation of MWCNT-PhS-Au Hybrid Materials. The phenylthiol functionality of the MWCNT-PhSH provides an anchoring point for attachment of Au NPs and Au NRs. To further assess the use of the MWCNT-PhSH as templates for metal immobilization, we treated them with pregrown spherical Au NPs or anisotropic Au NRs. Scheme 2 outlines the principle of the procedure.

Briefly, the premade CTAB-stabilized metallic materials were first isolated and characterized by TEM and UV−vis spectroscopy (Supporting Information, Figures S3 and S4). The original Au NPs were found to have an average diameter of 3.5 nm while the Au NRs were obtained in a 2.1 aspect ratio. The immobilization of these materials on the nanotube surface was carried out by mixing them with the MWCNT-PhSH to allow for the formation of Au−S bonds. A secondary seed-mediated growth of immobilized Au NPs into Au NRs was also conducted.[32]

Figure 4A illustrates a typical TEM image of the resulting hybrid material. Apparently, the Au NPs pack quite densely (~25 Au NPs per 100 nm CNT length on average) yet are still separated as individual spheres on the MWCNT-PhSH. The particles appear not to fuse or grow in the deposition process. This result substantiates the above-described characterization of MWCNT-PhSH, that is, that thiophenol sites prevail on the MWCNT structure after the reductive degradation of MWCNT-$(PhSSPh)_x$. In addition, we may assume that most of the Au NPs on the MWCNT surface are attached through Au−S bonds since little or no metal immobilization was observed if the pristine MWCNT was employed in the deposition process.

The procedure of attaching the NPs onto what is essentially a single layer of covalently attached thiophenol groups allows for an intimate connection of the metal and carbon material. The corresponding control experiments using the disulfide

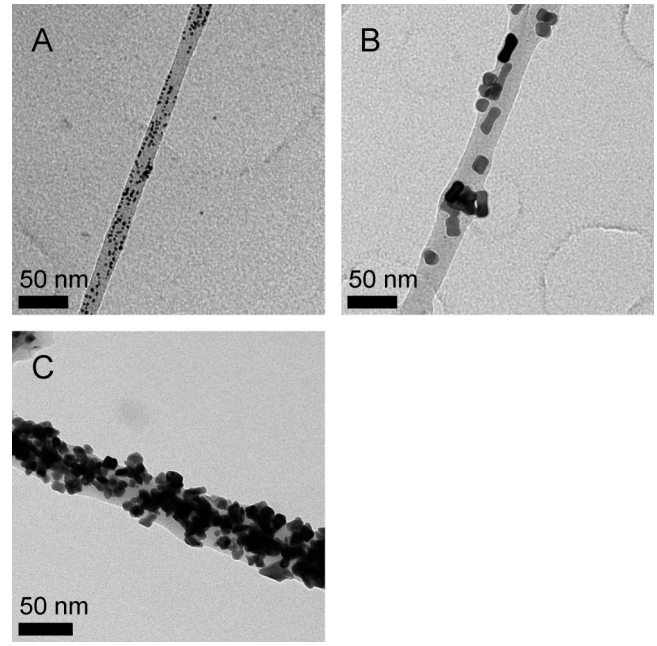

Figure 4. TEM images of the MWCNT-PhS-Au hybrids: Au NP immobilized on the surface of MWCNT-PhSH (A) and preformed Au NR immobilized on the surface of MWCNT-PhSH (B) and Au NRs seed-grown from the MWCNT-PhS-Au NP material (C).

multilayered MWCNT-$(PhSSPh)_x$ reveals essentially no metal immobilization. This observation is surprising considering that disulfides are expected to react with Au surfaces and particles, but it is in line with the electrochemical experiments. As a result of the weak surface plasmon absorption observed for the premade Au NPs (Supporting Information, Figure S3), UV−vis spectroscopy on the MWCNT-PhS-Au NP hybrid material is featureless and as such does not offer a clear statement of the presence or orientation of the Au NPs on the nanotube surface.

In an analogous manner, assembly of preformed Au NRs on the MWCNT-PhSH was accomplished. Figure 4B illustrates a TEM image of the assembled hybrid, in which the Au NRs are clearly resolved. A more highly Au NR functionalized MWCNT may be obtained in two steps through a secondary seed-mediated growth using the MWCNT-PhS-Au NP hybrid as a template; Figure 4C shows a TEM image of this material. Notably because of the relatively large initial density of Au NPs, only a part of the individual Au NRs are distinguishable. The material essentially becomes a gold-coated nanotube.

UV−vis spectroscopy allows for an identification of the presence of the Au NRs on the hybrid materials. When compared to the spectrum of the freely diffusing Au NRs (Supporting Information, Figure S4; $\lambda_{transverse} = 535$ and $\lambda_{longitudinal} = 690$ nm), a distinct red-shift of both the transverse and longitudinal surface plasmon band is observed for both the hybrid obtained from the pregrown Au-NRs (Supporting Information, Figure S5; $\lambda_{transverse} = 616$ and $\lambda_{longitudinal} = 765$ nm) and that obtained through the two-step growth onto MWCNT-PhS-Au NP (Supporting Information, Figure S6; $\lambda_{transverse} = 605$ and $\lambda_{longitudinal} = 940$ nm). This observation is a testimony of the intimate relationship between the

individual Au NRs on the MWCNT surface, leading to an apparent coupled surface plasmon absorption.[45]

Conclusion

In summary, we have devised a diazonium salt-based strategy to form first a dense multilayer of diphenyl disulfide on the surface of both SWCNTs and MWCNTs. The multilayer could then be degraded reductively to a phenylthiol functionality in, or close to, single layer fashion. This radical-based "formation−degradation" approach is unique in the sense that it allows the formation of a thin well-defined reactive layer. The materials were characterized by TEM, TGA, XPS, and electrochemical desorption experiments that allowed for support of the intended mechanism and TGA and XPS to estimate the extent of functionalization. In UV−vis spectroscopy, the disappearance of the Van Hove singularities of the SWCNT after the sidewall functionalization is consistent with the break up of the conjugated π system and verifies covalent sidewall functionalization.

Our functionalization method is essentially a one-pot procedure since the involved reactions are carried out without intermediate workup. The MWCNT-PhSH and SWCNT-PhSH materials can self-assemble on Au surfaces, which may turn out to be favorable for the development of nanoscale devices. The versatility of the thiolated CNTs also allows the immobilization of Au NPs or Au NRs, and we expect that this method can be extended to create nanosystems such as catalyst NPs and quantum dots. Such hybrid nanostructures may be used in catalytic, electronic, optical, and sensor applications.

Acknowledgment. We thank Lene Hubert from Risø National Laboratory for performing the XPS analysis and Carsten Bloch from Grundfos Management A/S for recording the TGA curves.

Supporting Information Available: TGA, linear sweep voltammogram, TEM, and UV−vis spectra (PDF). This material is available free of charge via the Internet at http://pubs.acs.org.

CM800954T

(45) Thomas, K. G.; Barazzouk, S.; Ipe, B. I.; Joseph, S. T. S.; Kamat, P. V. *J. Phys. Chem. B* **2004**, *108*, 13066–13068.